Electronic Supplementary Material (ESI) for Inorganic Chemistry Frontiers.

Metallic tin nanodots inducing interfacial adsorption-insertion mechanism for carbon nano-honeycombs with enhanced sodium storage

Xuepeng Ni[1], Kunming Li[1], Xin Wang[2], Xian Zhao[3], Dong Li[1], Huifang Chen[1], Qilin Wu[1*], Anqi Ju[1*] and Meifang Zhu[1]

[1] *College of Materials Science and Engineering & State Key Laboratory for Modification of Chemical Fibers and Polymer Materials, Donghua University, Shanghai 201620, China*

[2] *Songshan Lake Materials Laboratory, Dongguan 523808, China*

[3] *Department of Chemistry, University of Cincinnati, Cincinnati, Ohio 45221, United States*

Corresponding author:
Name: Anqi Ju
E-mail: anqiju@163.com

Experiment section

Materials

Cyanuric acid (CA) was purchased by Bide Pharmatech Ltd., Shanghai, China. Melamine (MA), glucose and ethanol were commercially supplied by Sinopharm Chemical Reagent Co., Ltd., Shanghai, China. The $SnCl_4 \cdot 5H_2O$ and Dimethyl sulfoxide (DMSO) were obtained from Aladdin reagent (Shanghai) Co., Ltd., China. All chemicals were directly used without any further purification.

Preparation of N-doped carbon nano-honeycombs modulated by metallic tin nanodots

Both MA (3.0 g) and $SnCl_4 \cdot 5H_2O$ (3.0 g) were dissolved in 120 mL of DMSO under sonication to form solution A, and CA (3.2 g) was dissolved in 60 mL of DMSO under sonication to form solution B. Then, the solution A and B were mixed directly and stirred for 10 min to obtain a white precipitate at room temperature. Finally, the white precipitate was collected by centrifugation, washed with DMSO, H_2O and ethanol several times, and dried at 60 °C in a vacuum overnight to obtain a white powder with Sn (denoted as 3-Sn-MCA). The mixture consisting of the as-prepared 3-Sn-MCA and glucose (4:1, wt%/wt%) was transformed to the tubular furnace for heating at 150 ℃ for 2 h, and followed by carbonization at 900 ℃ for 1 h with a heating rate of 2 ℃/min to achieve carbon nano-honeycombs modulated by metallic tin nanodots (denoted as 3-Sn/N-CNs) under nitrogen atmosphere during the whole process.

For comparison, the various N-doped carbon nanocages anodes modified with Sn nanodots were prepared by adjusting the $SnCl_4 \cdot 5H_2O$ added mass. The mass of $SnCl_4 \cdot 5H_2O$ added was 0 g, 2.1 g, 4.0 g and 5.0 g to get N-doped carbon nano-honeycombs anodes modulated by metallic tin nanodots and other procedure was similar with 3-Sn/N-CNs, the resultants were named as N-CNs, 2-Sn/N-CNs, 4-Sn/N-CNs and 5-Sn/N-CNs, respectively.

Structural and Morphological Characterization

Both the field emission scanning electron microscope (FESEM, SU-8010) and high-resolution transmission electron microscope (HRTEM, JEM-2100F) were used to

analyze the morphology and microstructure of three as-prepared samples. The structure, surface chemical species, and degree of graphitization and defects of all the samples were measured by X-ray diffraction (XRD, Rigaku D/max 2550 V diffractometer), X-ray photoelectron spectroscopy (XPS, Escalab 250Xi) and Raman spectroscopy (inVia-Reflex), respectively. The nitrogen adsorption-desorption isotherms and pore size distribution of the samples were achieved using the fully automatic specific surface area and pore size tester (Micro ASAP2046) at 77 K.

Electrical and Electrochemical Measurements

The electrochemical measurements of N-CNs and 3-Sn/N-CNs were performed in CR2032 coin-type cells. The 80 wt% active materials, 10 wt% super P and 10 wt% polyvinylidene difluoride (PVDF) binder were absolutely dissolved in N-methyle-2-pyrrolidone (NMP) solvent, and pasting the obtained homogeneous slurry onto the copper foil. Then the copper foil coated with active materials was transferred to the vacuum oven at 60 °C for 12 h and was cut into many copper pieces with a diameter of 12 mm as the working electrode. The specific capacity was calculated according to the total mass of the active materials. Both the sodium metal and glass fiber (GF/D, from Whatman) served as the counter electrodes and the separator, respectively. The applied electrolyte was 1 M $NaPF_6$ dissolved in dimethyl ether (DME). Cyclic voltammograms (CV) test (0.01-2 V, *vs* Na/Na^+) was carried out with distinct scan rates by using an electrochemical workstation (Ivium-V01320). The battery tester (LAND-CT2001A) was employed to test the cycling and rating performance of three samples at various current densities (0.01-2 V, *vs* Na/Na^+). Electrochemical impedance spectra (EIS) were characterized with a frequency range between 100 kHz and 0.01 Hz by using an electrochemical workstation (Ivium-V01320). For full cells preparation, the 3-Sn/N-CNs anode is pre-sodiated in a half-cell for 5 cycles at 0.1 A/g in voltage range of 0.01~3 V to ensure the formation of a stable solid electrolyte interphase film. Then the $Na_3V_2(PO_4)_2O_2F$ is used as cathode to assemble the sodium-ion full cell. The electrolyte and separator are the same as above.

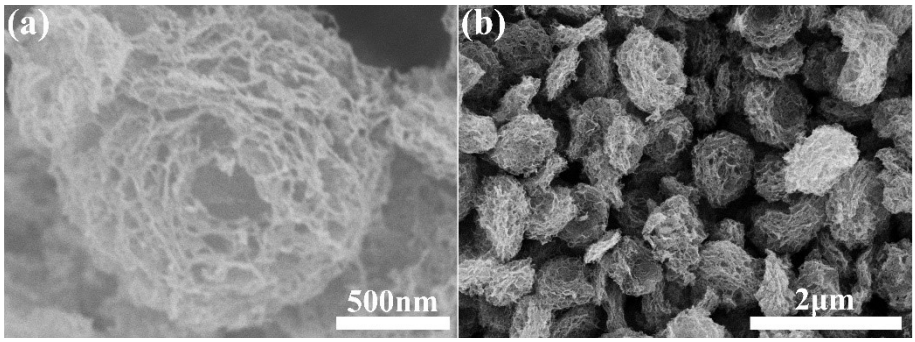

Fig. S1. (a-b) SEM images of N-CNs.

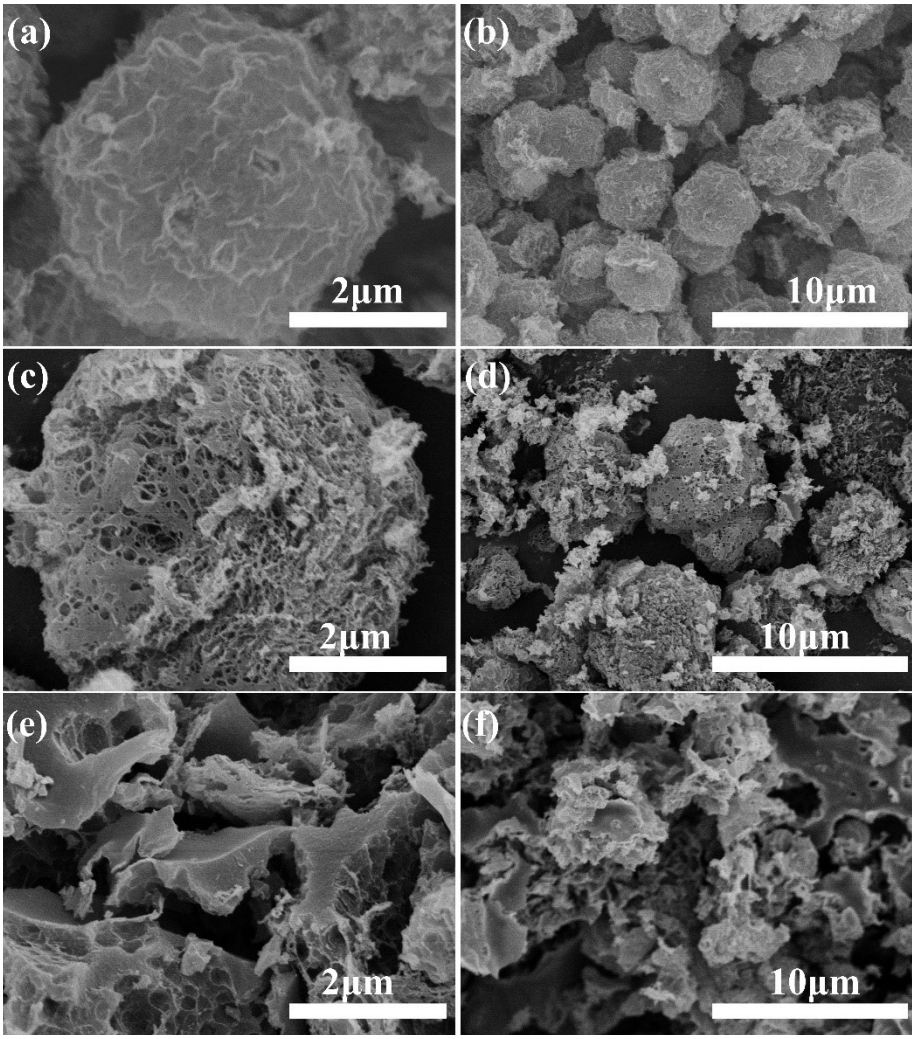

Fig. S2. SEM images of 2-Sn/N-CNs (a-b), 4-Sn/N-CNs (c-d) and 5-Sn/N-CNs (e-f).

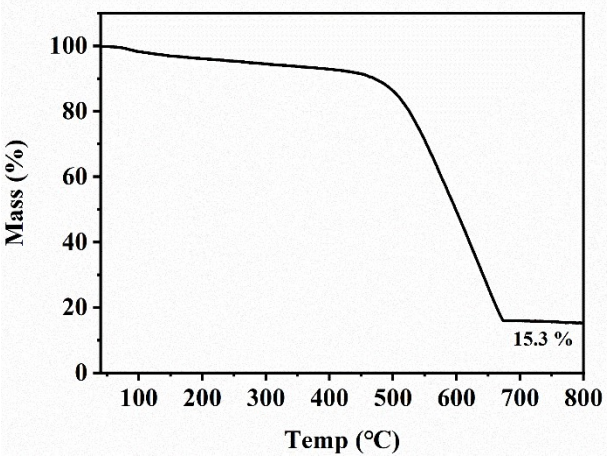

Fig. S3 The TGA curve of 3-Sn/N-CNs.

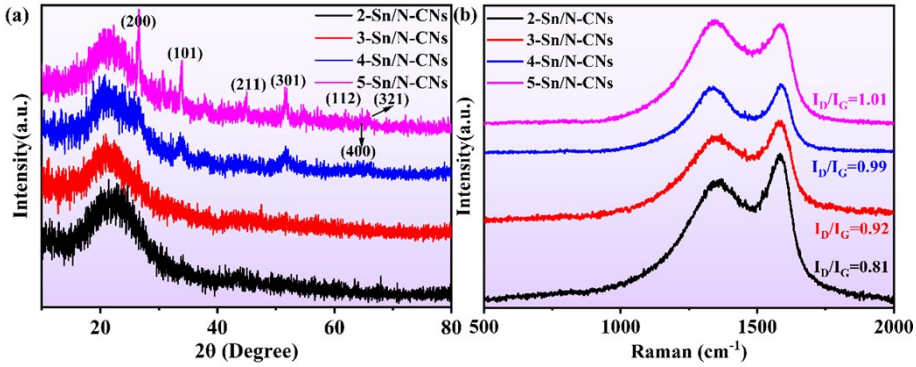

Fig. S4. (a) XRD pattern and (b) Raman spectra of 2-Sn/N-CNs, 3-Sn/N-CNs, 4-Sn/N-CNs and 5-Sn/N-CNs.

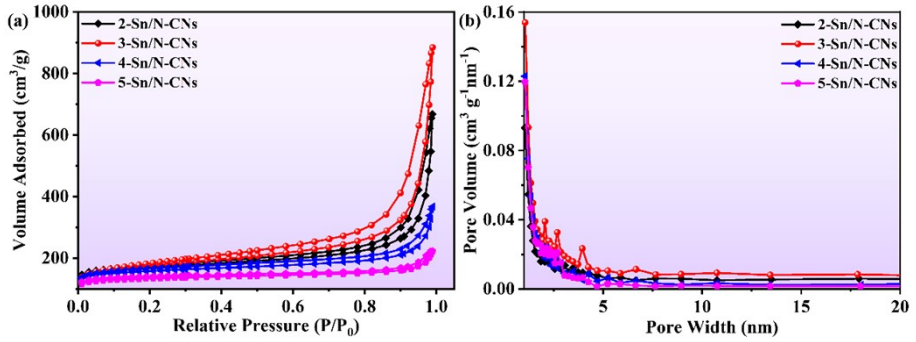

Fig. S5. (a) N_2 adsorption-desorption isotherms and (b) the pore-size distribution curves of 2-Sn/N-CNs, 3-Sn/N-CNs, 4-Sn/N-CNs and 5-Sn/N-CNs.

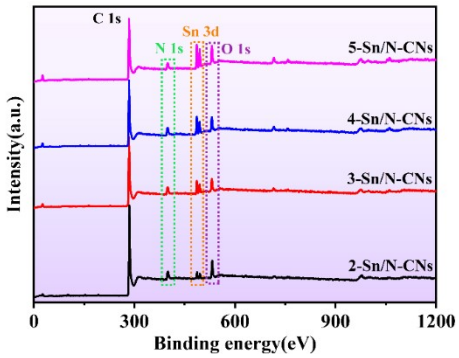

Fig. S6. XPS survey spectra of 2-Sn/N-CNs, 3-Sn/N-CNs, 4-Sn/N-CNs and 5-Sn/N-CNs.

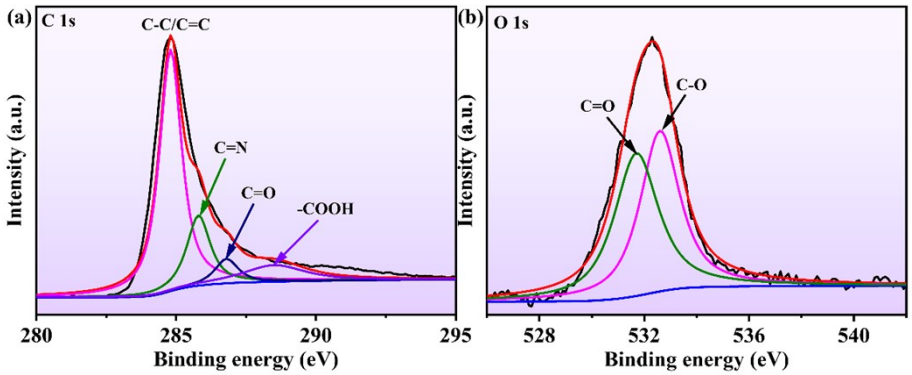

Fig. S7. High-resolution XPS spectra of 3-Sn/N-CNs: (a) C 1s, (b) O 1s.

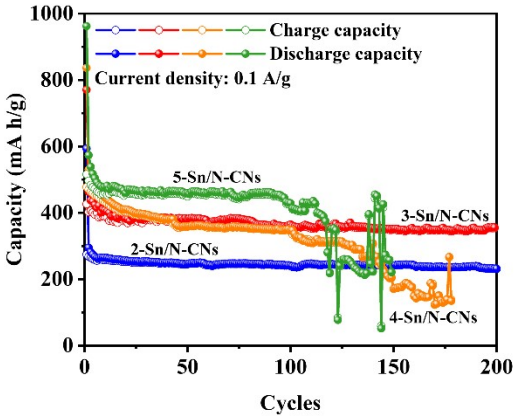

Fig. S8 The cycling performance at 0.1 A/g of the 2-Sn/N-CNs, 3-Sn/N-CNs, 4-Sn/N-CNs and 5-Sn/N-CNs.

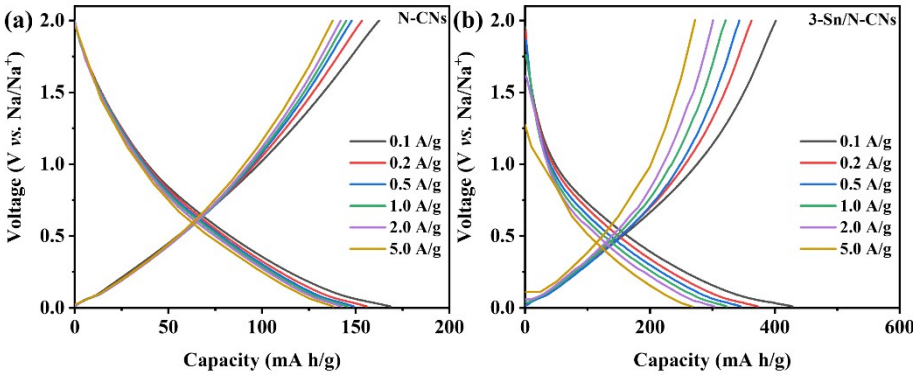

Fig. S9 The galvanostatic discharge/charge profiles of (a) N-CNs and (b) 3-Sn/N-CNs at various current densities.

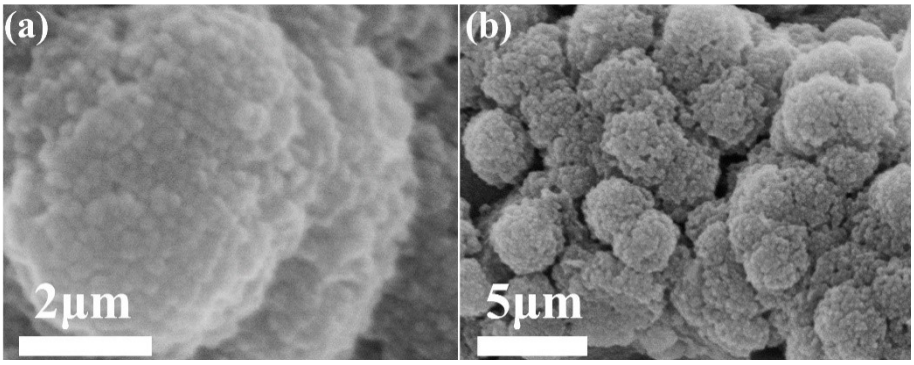

Fig. S10 The SEM images of 3-Sn/N-CNs after cycles.

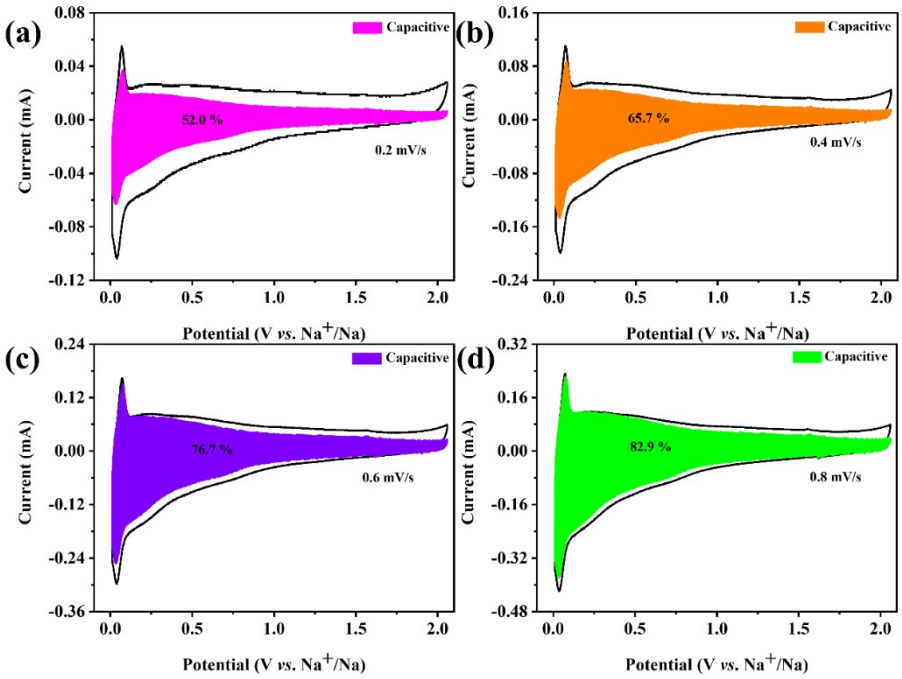

Fig. S11. The capacitive contribution ratio of 3-Sn/N-CNs at different scan rates.

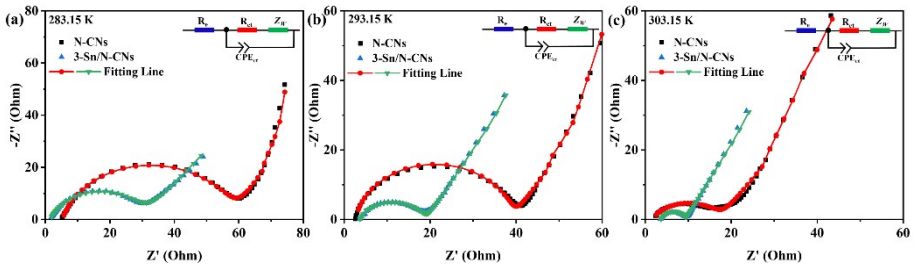

Fig. S12 Electrochemical impedance spectra of both N-CNs and 3-Sn/N-CNs at 283.15 K (a), 293.15 K (b) and 303.15 K (c). Based on the equivalent circuit exhibited in the inset of (a-c), the fitted lines (solid lines) were achieved.

Table S1. Comparison of the 3-Sn/N-CNs anode with recently reported carbon anodes for sodium-ion half cells.

Materials	current density (A/g)	capacity (mA h/g)	cycling	Ref
MPC	5	200	5000	1
NCNFs-IWNC800	5	146	5000	2
3D-PC-800	5	120	1000	3
NP-HPCS	5	120	5000	4
CC700	1	105	8000	5
N-HC	5	101.4	10000	6
S-N/C a	1.0	211	1000	7
HARC800	1	119	1000	8
WSC-1000	1	182	1500	9
NS-CNRs-700	1	230	3000	10
NPCs-4	5	251.3	10000	**This work**

Table S2. Transfer resistances (R_{ct}) and activation energy of both N-CNs and 3-Sn/N-CNs.

Samples	283.15 K (Ω)	293.15 K (Ω)	303.15 K (Ω)	Activation energy(kJ/mol)
N-CNs	53.82	36.7	16.54	59.3
3-Sn/N-CNs	29.08	16.09	5.48	41.9

References

1 Y. Tong, Y. Wu, Z. Liu, Y. Yin, Y. Sun and H. Li, Fabricating multi-porous carbon anode with remarkable initial coulombic efficiency and enhanced rate capability for sodium-ion batteries, *Chin. Chem. Lett.*, 2023, **34**, 107443.

2 W. Zhao, X. Hu, S. Ci, J. Chen, G. Wang, Q. Xu and Z. Wen, N-Doped Carbon Nanofibers with Interweaved Nanochannels for High-Performance Sodium-Ion Storage, *Small*, 2019, **15**, 1904054.

3 C. Zhou, D. Wang, A. Li, E. Pan, H. Liu, X. Chen, M. Jia and H. Song, Three-dimensional porous carbon doped with N, O and P heteroatoms as high-performance anode materials for sodium ion batteries, *Chem. Eng. J.*, 2020, **380**, 122457.

4 H. Wang, J.-L. Lan, H. Yuan, S. Luo, Y. Huang, Y. Yu, Q. Cai and X. Yang, Chemical Grafting-derived N, P Co-doped Hollow Microporous Carbon Spheres for High-Performance Sodium-ion Battery Anodes, *Appl. Surf. Sci.*, 2020, **518**, 146221.

5 R. Hao, Y. Yang, H. Wang, B. Jia, G. Ma, D. Yu, L. Guo and S. Yang, Direct chitin conversion to N-doped amorphous carbon nanofibers for high-performing full sodium-ion batteries, *Nano Energy*, 2018, **45**, 220-228.

6 X. Hu, X. Sun, S. J. Yoo, B. Evanko, F. Fan, S. Cai, C. Zheng, W. Hu and G. D. Stucky, Nitrogen-rich hierarchically porous carbon as a high-rate anode material with ultra-stable cyclability and high capacity for capacitive sodium-ion batteries, *Nano Energy*, 2019, **56**, 828-839.

7 J. Yang, X. Zhou, D. Wu, X. Zhao and Z. Zhou, S-Doped N-Rich Carbon Nanosheets with Expanded Interlayer Distance as Anode Materials for Sodium-Ion Batteries, *Adv. Mater.*, 2017, **29**, 1604108.

8 Z. Jiang, C. Zhang, X. Qu, B. Xing, G. Huang, B. Xu, C. Shi, W. Kang, J. Yu and S. W. Hong, Humic acid resin-based amorphous porous carbon as high rate and cycle performance anode for sodium-ion batteries, *Electrochim. Acta*, 2021, **372**, 137850.

9 Q. Li, Y.-N. Zhang, S. Feng, D. Liu, G. Wang, Q. Tan, S. Jiang and J. Yuan, N, S self-doped porous carbon with enlarged interlayer distance as anode for high performance sodium ion batteries, *Int. J. Energy Res.*, 2021, **45**, 7082-7092.

10 A. Hu, S. Jin, Z. Du, H. Jin and H. Ji, NS codoped carbon nanorods as anode materials for high-performance lithium and sodium ion batteries, *J. Energy Chem.*, 2018, **27**, 203-208.